Simultaneous CCD Photometry of Two Eclipsing Binary Stars in Pegasus—Part 1: KW Pegasi

Kevin B. Alton
UnderOak Observatory, 70 Summit Avenue, Cedar Knolls, NJ 07927; kbalton@optonline.net

Received December 5, 2012; revised January 3, 2013; accepted January 3, 2013

Abstract The coincidental location of BX Peg and KW Peg in the same field-of-view captured by the primary imaging system at UnderOak Observatory (UO) provided an opportunity to study both variable stars from the same exposures. Herein new findings for the eclipsing binary KW Peg will be presented while those from BX Peg will be discussed in a separate paper (Part 2). KW Peg, described as an "Algol type" eclipsing variable (P = 0.816402 d), is only reported in a single work published over twenty years ago. Photometric data collected in three bandpasses (B, V, and I_c), produced eight new times of minimum for KW Peg. These were used to update the linear ephemeris and further analyze potential changes in orbital periodicity by examining the available history of eclipse timings. In addition, synthetic fitting of light curves by Roche modeling was accomplished with programs employing the Wilson-Devinney code. Results from the present study provide a reasonable case for classifying KW Peg as a short-period RS CVn eclipsing binary rather than Algol-like. The primary star in KW Peg would appear to be a late stage G9V-K0V dwarf whereas the secondary is a slightly cooler K0-K1 companion. The eclipse-timing diagram for KW Peg is quite simple and indicates that, on average, the orbital period for this system has remained fairly constant over the past two decades.

1. Introduction

KW Peg was first detected as a variable by De Young (1991). The shape of the corresponding light curve suggested a semi-detached Algol-type eclipsing binary; however, aside from times-of-minimum from a number of different sources, no comprehensive analysis of this variable target is reported in the literature. The initial reported (De Young 1991) orbital period (0.816384 d) closely agrees with that published by Kreiner (2004).

2. Observations and data reduction

2.1. Astrometry

Images of KW Peg were automatically matched against the standard star fields (UCAC3) provided in MPO CANOPUS v10.3.0.2 (Minor Planet Observer 2010) and then rotated and scaled as necessary. Plate constants were

internally calculated which convert X/Y coordinates of a detected object to a corresponding right ascension and declination.

2.2. Photometry

A summary of CCD photometric session dates (UTC) is tabulated below for campaigns conducted in 2008 and 2011.

2008	2011	
October	October	November
8, 10, 12, 13, 16, 18, 19, 20, 24, 27, 31	6, 7, 8, 9, 10	3, 8

Equipment included a 0.2-m catadioptic telescope with an SBIG ST 402ME CCD camera mounted at the primary focus. Automated multi-bandwidth imaging was performed with SBIG photometric B, V, and I_c filters manufactured to match the Bessell prescription. Since accurate timing for each image is critical, the computer clock was updated automatically (Dimension 4; http://www.thinkman.com/dimension4/) via the U.S. Naval Observatory Time Server immediately prior to each session. In general, image acquisition (lights, darks, and flats) was performed using CCDSOFT v5 (Software Bisque 2011) while calibration and registration were accomplished with AIP4WIN v2.3.1 (Berry and Burnell 2005). MPO CANOPUS provided the means for further photometric reduction using the same five non-varying comparison stars to ultimately calculate ephemerides and orbital periods. No color or air mass corrections were applied since images were only taken above 30° altitude (airmass < 2.0), which minimizes error due to differential refraction and color extinction. The exposure time for all filters was 45 seconds during the 2008 campaign but increased in 2011 to 90 seconds for B and 60 seconds for V and I_c. Instrumental readings were reduced to catalogue-based magnitudes using the MPOSC3 reference star fields built into MPO CANOPUS. Almost all stars in MPOSC3 also have $BVRI_c$ magnitudes derived from 2MASS J–K magnitudes; these have an internal consistency of ±0.05 mag. for V, ±0.08 mag. for B, ±0.03 mag. for I_c, and ±0.05 mag. for B–V (Warner 2007).

2.3 Light curve analyses

Roche-type modeling was performed using BINARY MAKER 3 (Bradstreet and Steelman 2002), WDWINT v5.6a (Nelson 2009a), and PHOEBE v.31a (Prša and Zwitter 2005), the latter two of which employ the Wilson-Devinney (W-D) code (Wilson and Devinney 1971; Wilson 1979). BINARY MAKER 3 (BM3) is a commercial application whereas PHOEBE (http://phoebe.fiz.uni-lj.si/) and WDWINT (http://members.shaw.ca/bob.nelson/software1.htm) are freely available GUI implementations of the W-D modeling code. 3-D spatial renderings of KW Peg were also produced by BM3 once each model fit was finalized. Times of minimum (ToM) were estimated using the method of Kwee and van Woerden (1956) as implemented in MINIMA V25c (Nelson 2007).

3. Results and discussion

3.1. Photometry

Five stars in the same FOV as KW Peg were selected to calculate the relative change in flux and derive catalogue-based (MPOSC3) magnitudes using the "Comp Star Selector" feature in MPO CANOPUS (Table 1). The difference in magnitude over time from each comparison star against the averaged magnitude yielded a narrow range of values with no obvious trend; variability was generally within ±0.015 mag. for V and I_c filters and ±0.03 for B passband.

3.2. Ephemerides

3.2.1 Light curves from 2008 campaign

Photometric observations in B (n = 878), V (n = 884), and I_c (n = 891) filters were folded to produce light curves that spanned 23 days (Figure 1). These observations included four new ToM values in each bandpass. No meaningful color dependencies emerged; therefore the timings from all three filters were averaged for each session (Table 2). Initially seeded with the orbital period (0.816402 d) posted at the Mt. Suhora Astronomical Observatory website (Kreiner 2004), the Fourier analysis routine (FALC) in MPO CANOPUS provided a period solution for all the data. The corresponding linear ephemeris (Equation 1) from the 2008 campaign alone was determined to be:

$$\text{Min. I (hel.)} = 2454766.5239\ (10) + 0.8164109\ (1)\ E \qquad (1)$$

3.2.2 Light curves from 2011 campaign

Photometric observations in B (n = 634), V (n = 645), and I_c (n = 652) passbands were folded by filter to produce light curves that spanned 32 days of imaging (Figure 2). These observations included four new ToM values in each bandpass (Table 2). As described above with the 2008 light curves, Fourier analysis yielded the following linear ephemeris (Equation 2) for the 2011 data collected at UO:

$$\text{Min. I (hel.)} = 2455873.5661\ (16) + 0.8164109\ (1)\ E \qquad (2)$$

Each of these periods was calculated using fairly short sampling times (< 33 days). Fourier analysis of pooled (2008 and 2011) light curve data extends the baseline period to 1,126 days, thereby improving the robustness of the period estimate. The resulting linear ephemeris (Equation 3) compares favorably with the limited number of values reported since De Young (1991).

$$\text{Min. I (hel.)} = 2455873.5661\ (16) + 0.8164020\ (1)\ E \qquad (3)$$

As is standard practice at UnderOak Observatory (UO), all period determinations were independently confirmed using PERANSO v2.5 (CBA Belgium Observatory 2011) by applying periodic orthogonals (Schwarzenberg-Czerny 1996) to fit

observations and analysis of variance (ANOVA) to evaluate fit quality. In toto, five new primary (p) and three new secondary (s) minima were recorded during this investigation. These eight minima along with additional values cited in AAVSO, IBVS, OEJV, BBSAG, and B.R.N.O. publications were used to prepare these data for period analysis (Table 3). The reference epoch (Kreiner 2004) used to calculate eclipse timing (ET) residuals was defined by the following linear ephemeris (Equation 4):

$$\text{Min. I (hel.)} = 2452500.1930\ (2) + 0.81640201\ (8)\ E \qquad (4)$$

The progression of orbital periodicity over time can be visualized by plotting the difference between the observed eclipse times and those predicted by the reference epoch against the period cycle number (Figure 3). More commonly called an observed minus computed (O–C) diagram, this generalized term fails to exactly inform the reader about which variables are being analyzed. Going forward in this paper the term eclipse timing or ET diagram will be used instead. The ET diagram for KW Peg (Figure 3) proved to be a quite simple in that nearly all observations fall within a straight line relationship. Accordingly, the latest linear ephemeris (Equation 5) was calculated from linear least squares fitting of data acquired between 1990 and 2011:

$$\text{Min. I (hel.)} = 2455873.5657\ (2) + 0.81640193\ (8)\ E \qquad (5)$$

As expected from this binary system which has exhibited a constant orbital period thus far, values obtained from the reference epoch in 2002 (Kreiner 2004), pooled (2008 and 2011) light curve data, and that predicted from the ET diagram using all data (1990–2011) are internally consistent (P = 0.816402 d).

3.3 Spectral classification

Folded light curves from 2008 and 2011 were similar enough in each filter to combine prior to modeling with BM3 and PHOEBE. In retrospect, the similarity between these two epochs is not unexpected, given that evidence from the ET diagram (Figure 3) suggests no remarkable changes have occurred over the past twenty-one years. The associated light curve shapes are consistent with a detached binary. Minima appear to be equally separated and, unless our vantage point is coincidently staring directly down the semi-major axis of an elliptical system, this finding suggests a circular orbit for this system. Both peaks had very similar widths, further arguing against an elliptical orbit. No source was found in the literature which posited a spectral class for this binary system. It was therefore necessary to piece together assorted data produced at UO and from several other survey catalogues in order to make an informed guess regarding the classification, and by inference, its temperature. The effective temperature ($Teff_1$) of the primary was initially estimated from B–V magnitudes determined at UO during quadrature (0.25P and 0.75P). This color index (0.733) corresponds to the effective temperature (5462 K; log = 3.737) of

a G8 main sequence star (Flower 1996; Harmanec 1988). Similar color index data calculated from other surveys (Table 4) suggest a potentially cooler system ranging between G8 and K2V. Therefore, Roche modeling of this system was initiated using a $Teff_1$ value (5260 K) midway between G8 and K2 spectral classes estimated for KW Peg (Table 4).

3.4 Roche modeling of combined KW Peg light curve data from the 2008 and 2011 campaigns

Before attempting to model light curve data from KW Peg additional assumptions had to be made regarding the physical makeup of this binary system. As mentioned before, the light curve shape suggests that KW Peg is most likely a detached binary in which stellar companions move around each other in a circular orbit (Min I and Min II separated by 0.5P). In the absence of any mass ratio data in the literature derived from radial velocity experiments, a starting point for q (m_1/m_2) was guesstimated as follows. Unlike many contact binaries, in well-detached systems the poor correlation between q, Ω_1, Ω_2, and other parameters precludes the possibility of deriving a reliable photometric mass ratio (Terrell and Wilson 2005). Assuming that KW Peg is on the main sequence, its putative spectral class (G9V-K0V) provides a hint regarding its mass (usually measured in solar masses, $M_\odot$). The relationship between spectral class and mass have been conveniently tabulated by Harmanec (1988) and in this case, the primary star in KW Peg is estimated to be less massive than Sol ($\sim 0.93\ M_\odot$). The comparative intensity of Min I and Min II in each bandpass also suggests that the size or luminosity of the secondary is probably not greatly different than the primary star, so q = 1 was initially adopted for modeling purposes.

Phased V-band light curve data that had been normalized with respect to flux were used for preliminary Roche modeling by BM3. Starting points for the Roche potentials ($\Omega_1 \approx 5.3$ and $\Omega_2 \approx 4.9$) were adopted according to the strategy proposed by Kang (2010) in which V364 Cas (Nelson 2009b) was used as the reference for a similarly shaped light curve from a detached system. Values for $Teff_1$ (5260 K) and a mass ratio (q = 1) were held constant while iteratively adjusting the effective temperature of the cooler secondary ($Teff_2$), inclination (i), and surface potentials (Ω_1 and Ω_2) until a reasonable fit to the model was obtained. Bolometric albedo ($A_{1,2}$ = 0.5) and gravity darkening coefficients ($g_{1,2}$ = 0.32) for cooler stars with convective envelopes were assigned according to Rucinski (1969) and Lucy (1967), respectively. Following any Teff change to either star, new logarithmic limb darkening coefficients (x_1, x_2, y_1, y_2) were interpolated according to van Hamme (1993). Thereafter, model fitting in PHOEBE employed phased data which had been transformed into catalogue-based magnitudes. A_1, A_2, g_1, g_2, and $Teff_1$ were fixed parameters whereas values for Ω_1 (5.2), Ω_2 (5.1), i (80°) and T_2 (5000 K), initially obtained from BM3 along with passband specific luminosity, phase shift, x_1, x_2, y_1, and y_2, were iteratively

adjusted using differential corrections (DC) to achieve a simultaneous minimum residual fit of all (B, V, and I_c) photometric observations. It should be noted that light curves from KW Peg are noisier in all passbands compared to other binary systems that have been imaged with similar or lower apparent magnitudes using the same equipment at UO. Since light curves from KW Peg and BX Peg (Alton 2013), a known W UMa binary, were reduced using the same ensemble of stars (Table 1), a direct comparison of residual mean error from the best fit Roche models (B, V, and I_c) consistently revealed higher (~17%) photometric variability for KW Peg. Although not compelling, it led this investigator to consider the possibility that this detached binary belongs to the short period RS CVn group of eclipsing stars. This observation may be related to the well-documented coronal and/or chromospheric activity of these variables (Heckert *et al.* 1998; Budding and Zeilik 1987).

The reader should, however, be advised that a large number of assumptions are required to nominate KW Peg as a potential member of the short-period RS CVn group of binaries. A defining characteristic (Hall 1976) of RS CVn systems is excess emission centered on the Ca II (H and K) and Hα lines so that a high resolution spectroscopic study is ultimately needed to unambiguously define the mass ratio, rotational velocity, and classification of this system. Nonetheless, the best fit unspotted model values for $Teff_1$ (5260 K) and $Teff_2$ (5047 K) are consistent with a well detached binary composed of a G9-K0V primary and a K0-K1 secondary. These spectral classes are fairly typical of those observed in other short-period RS CVn variables. At least during 2008 and 2011, the light curves from KW Peg are quite similar but do exhibit asymmetry relative to the clean unspotted curve fits, suggesting the putative spot has been stable for an extended period of time. By contrast, many other RS CVn stars feature prominent cool spots on the primary and/or evidence of coronal flares which can result in dramatic out-of-eclipse distortions in the light curves (Hilditch 2001) which change over much shorter time scales (Hempelmann *et al.* 1997).

Finding a spotted solution that matched the out-of-eclipse portion of the light curve and meaningfully enhanced the overall model fit proved to be less than completely successful. One approach which improved the curve fit was to position a hot spot on the secondary facing the primary star (Figure 4). Mathematical goodness-of-fit aside, this hot spot solution is difficult to defend considering the following factors. Since KW Peg appears to be a well-detached system, mass transfer which could lead to a hot spot formed by direct impact of an accretion stream is highly unlikely. Furthermore, the straight line relationship in the ET diagram for KW Peg (Figure 3) rather than a parabolic response strongly argues against this possibility since the orbital period is not changing significantly. Secondly, although persistent (months to years) cool spots have been documented for some RS CVn stars, flares or hot spots tend to be much more transient (Osten *et al.* 2000). Unless by mere coincidence, a hot spot is unlikely to persist at the same location as suggested by the similarity

between the 2008 and 2011 light curves. Large crown-like polar spots are more commonly observed as enduring features in other RS CVn stars (Hatzes *et al.* 1996). This addition to the model (Figure 4) was not as effective as a hot spot at minimizing model error, but at least could be rationalized based on the known behavior of other RS CVn systems. Hence, only the clean synthetic light curve fits and those with a single cool spot are reproduced in Figures 5 (B mag.), 6 (V mag.), and 7 (I_c mag.). For the sake of completeness, a comparison of all light curve parameters and geometric elements obtained from Roche modeling is summarized in Table 5. Other multiple starspot combinations were attempted but none led to a convincing improvement over these synthetic curves.

4. Conclusions

CCD-based photometric data collected in B, V, and I_c produced eight new times of minimum for KW Peg. The linear ephemeris for this system was updated and potential changes in orbital periodicity assessed through the analysis of observed versus predicted eclipse timings. The ET diagram for KW Peg is relatively simple and indicates that the orbital period for this system has remained fairly constant over the past two decades. In addition, results from the present study provide a reasonable case for classifying KW Peg as a short-period RS CVn eclipsing binary rather than Algol-like but further observations will need to be made to confirm that classification. The primary star in KW Peg is proposed to be a G9V-K0V dwarf whereas its secondary companion is slightly cooler (K0-K1). The addition of a single cool or hot spot on either star failed to fully account for the out-of-eclipse asymmetry observed in all 2008 and 2011 light curves. Public access to any light curve data associated with this research can be obtained by request (mail@underoakobservatory.com)

5. Acknowledgements

This research has made use of the SIMBAD database, operated at Centre de Donnees astronomiques de Strasbourg, France. Times of minimum data published by B.R.N.O., IBVS, AAVSO, BAV-M, and BBSAG proved invaluable to the assessment of potential period changes. The diligence and dedication shown by all associated with these organizations is very much appreciated. Last, and certainly not least, I would like to thank Professor Dirk Terrell and an unknown referee for their selfless assistance in reviewing this study report and suggesting changes that have significantly improved the quality of this manuscript.

References

Agerer, F., and Hübscher, J. 2003, *Inf. Bull. Var. Stars*, No. 5484, 1.
Alton, K. B. 2013, *J. Amer. Assoc. Var. Star Obs.*, **41**, in press.
Beob. der Schweizerischen Astron. Ges. (BBSAG). 1994, *BBSAG Bull.*, No. 106, 1.
Berry, R., and Burnell, J. 2005, *Handbook of Astronomical Image Processing*, Willmann-Bell, Richmond.
Bradstreet, D. H., and Steelman, D. P. 2002, *Bull. Amer. Astron. Soc.*, **34**, 1224.
Brát, L., Zejda, M., and Svoboda, P. 2007, *Open Eur. J. Var. Stars*, **74**, 1 (*B.R.N.O. Contrib.*, No. 34).
Brát, L., *et al.* 2011, *Open Eur. J. Var. Stars*, **137**, 1 (*B.R.N.O. Contrib.*, No. 37).
Budding, E., and Zeilik, M. 1987, *Astrophys. J.*, **319**, 827.
CBA Belgium Observatory. 2011, Flanders, Belgium (http://www.cbabelgium.com/).
De Young, J. A. 1991, *Inf. Bull. Var. Stars*, No. 3579, 1.
Diethelm, R. 2010, *Inf. Bull. Var. Stars*, No. 5920,1.
Diethelm, R. 2012, *Inf. Bull. Var. Stars*, No. 6011, 1.
Dvorak, S.W. 2006, *Inf. Bull. Var. Stars*, No. 5677, 1.
Flower, P. J. 1996, *Astrophys. J.*, **469**, 355.
Hall, D. S. 1976, in *Multiple Periodic Variable Stars*, ed. W. S. Fitch, IAU Symp. 29, Reidel, Dordrecht, 287.
Harmanec, P. 1988, *Bull. Astron. Inst. Czechoslovakia*, **39**, 329.
Hatzes, A. P., Vogt, S. S., Ramseyer, T. F., and Misch, A. 1996, *Astrophys. J.*, **469**, 808.
Heckert, P. A., Maloney, G. V., Stewart, M. C., Ordway, J. I., Hickman, A., and Zeilik, M. 1998, *Astron. J.*, **115**, 1145.
Hempelmann, A., Hatzes, A. P., Kürster, M., and Patkós, L. 1997, *Astron. Astrophys.*, **317**, 125.
Hilditch, R. W. 2001, *An Introduction to Close Binary Stars*, Cambridge Univ. Press, New York.
Hübscher, J. 2005, *Inf. Bull. Var. Stars*, No. 5643, 1.
Hübscher, J. 2011, *Inf. Bull. Var. Stars*, No. 5984, 1.
Hübscher, J., and Lehmann, P. B. 2012, *Inf. Bull. Var. Stars*, No. 6026, 1.
Hübscher, J., Paschke, A., and Walter, F. 2005, *Inf. Bull. Var. Stars*, No. 5657, 1.
Hübscher, J., Paschke, A., and Walter, F. 2006, *Inf. Bull. Var. Stars*, No. 5731,1.
Hübscher, J., and Walter, F. 2007, *Inf. Bull. Var. Stars*, No. 5761, 1.
Kang, Y.-W. 2010, *J. Astron. Space Sci.*, **27**, 75.
Kotková, L., and Wolf, M. 2006, *Inf. Bull. Var. Stars*, No. 5676, 1.
Krajci, T. 2005, *Inf. Bull. Var. Stars*, No. 5592, 1.
Kreiner, J. M. 2004, *Acta Astron.*, **54**, 207.

Kwee, K. K., and Van Woerden, H. 1956, *Bull. Astron. Inst. Netherlands*, **12**, 327.
Lucy, L. B. 1967, *Z. Astrophys.*, **65**, 89.
Minor Planet Observer. 2010, MPO Software Suite (http://www.minorplanetobserver.com), BDW Publishing, Colorado Springs.
Nelson, R. H. 2007, Minima©2002–2006: Astronomy Software by Bob Nelson (http://members.shaw.ca/bob.nelson/software1.htm).
Nelson, R. H. 2009a, WDwint56a: Astronomy Software by Bob Nelson (http://members.shaw.ca/bob.nelson/software1.htm).
Nelson, R. H. 2009b, *Inf. Bull. Var. Stars*, No. 5884, 1.
Osten, R. A., Brown, A., Ayres, T. R., Linsky, J. L., Drake, S. A., Gagné, M., and Stern, R. A. 2000, *Astrophys. J.*, **544**, 953.
Parimucha, Š., Dubovský, P., Baludanský, D., Pribulla, T., Hambalek, L., Vanko, M., and Ogloza, W. 2009, *Inf. Bull. Var. Stars*, No. 5898, 1.
Pribulla, T., *et al.* 2005, *Inf. Bull. Var. Stars*, No. 5668, 1.
Prša, A. and Harmanec, P. 2010, *PHOEBE Manual: Adopted for PHOEBE 0.32*, Villanova Univ., Dept. of Astronomy and Astrophysics, Villanova, PA (http://phoebe.fmf.uni-lj.si/docs/phoebe_manual.pdf).
Prša, A., and Zwitter, T. 2005, *Astrophys. J.*, **628**, 426.
Ruciński, S. M. 1969, *Acta Astron.*, **19**, 245.
Samolyk, G. 2008, *J. Amer. Assoc. Var. Star Obs.*, **36**, 186.
Samolyk, G. 2010, *J. Amer. Assoc. Var. Star Obs.*, **38**, 183.
Schwarzenberg-Czerny, A. 1996, *Astrophys. J., Lett. Ed.*, **460**, L107.
Software Bisque 2011, Santa Barbara Instrument Group, Santa Barbara, CA.
Terrell, D., and Wilson, R. E. 2005, *Astrophys. Space Sci.*, **296**, 221.
van Hamme, W. 1993, *Astron. J.*, **106**, 2096.
Warner, B. 2007, *Minor Planet Bull.*, **34**, 113.
Wilson, R. E. 1979, *Astrophys. J.*, **234**, 1054.
Wilson, R. E., and Devinney, E. J. 1971, *Astrophys. J.*, **166**, 605.
Zasche, P., Uhlar, R., Kucáková, H., and Svoboda, P. 2011, *Inf. Bull. Var. Stars*, No. 6007, 1.
Zejda, M. 2004, *Inf. Bull. Var. Stars*, No. 5583, 1.
Zejda, M., Mikulásek, Z., and Wolf, M. 2006, *Inf. Bull. Var. Stars*, No. 5741, 1.

Table 1. Astrometric coordinates (J2000) and MPOSC3 catalogue magnitudes (V, B, and I_c) for KW Peg and five comparison stars used in this photometric study.

Star Identification	*R.A.* h m s	*Dec.* ° ′ ″	*MPOSC3*[a] *B mag.*	*MPOSC3 V mag.*	*MPOSC3* I_c *mag.*	*MPOSC3 (B–V)*
KW Peg	21 39 10.59	26 42 34.4	12.65–13.05[b]	11.9–12.3	11.08–11.44	0.805
C1	21 38 57.74	26 36 51.4	13.154	12.694	12.145	0.460
C2	21 39 00.59	26 38 10.4	13.327 (13.51)[c]	12.678 (12.77)[c]	11.95	0.649
C3	21 39 02.87	26 38 43.0	13.384 (13.37)[c]	12.287 (12.34)[c]	11.16 (11.20)[c]	1.097
C4	21 39 07.72	26 44 37.4	13.219	12.736	12.164	0.483
C5	21 39 00.86	26 44 58.8	13.88	13.044	12.151	0.836

Notes: a. MPOSC3 is a hybrid catalogue which includes a large subset of the Carlsberg Meridian Catalog (CMC-14) as well as the Sloan Digital Sky Survey (SDSS). b. Range of magnitudes in light curves for each variable. c. AAVSO comparison star magnitudes in parentheses.

Table 2. New times of minimum for KW Peg acquired at UnderOak Observatory.

Mean Computed Time of Minimum (HJD–2400000)[a]	*Error ±*	*UT Date of Observations*	*Type of Minimum*[a]
54755.5016	0.0010	16 Oct 2008	s
54757.5431	0.0007	18 Oct 2008	p
54759.5844	0.0008	20 Oct 2008	s
54766.5239	0.0010	27 Oct 2008	p
55842.5411	0.0019	08 Oct 2011	p
55844.5806	0.0011	10 Oct 2011	s
55868.6681	0.0013	03 Nov 2011	p
55873.5661	0.0016	08 Nov 2011	p

Note: a. s= secondary; p = primary.

Table 3. Recalculated eclipse timing residuals $(ETR)_2$ for KW Peg following simple linear least squares fit of residuals $(ETR)_1$ from the reference epoch and cycle number occurring between 1990 Sept 24 and 2011 Nov 08.

Time of Minimum (HJD–2400000)	*Type*	*Cycle Number*	$(ETR)_1$[a]	$(ETR)_2$	*Reference**
48158.5685	p	–5318	0.00138918	0.00034626	1
48160.6075	s	–5315.5	–0.00061584	0.00034606	1
48225.5099	p	–5236	–0.00217564	0.00033970	1
48225.5122	p	–5236	0.00012436	0.00033970	1
49250.5040	s	–3980.5	–0.00079919	0.00023922	2
52240.5777	p	–318	0.00053918	–0.00005392	3
52505.4998	s	6.5	0.00018694	–0.00007989	4
52510.3966	s	12.5	–0.00142512	–0.00008037	4
52521.4223	p	26	0.00284774	–0.00008145	5
52602.6530	s	125.5	0.00154774	–0.00008942	3
52878.5966	s	463.5	0.00126836	–0.00011647	6
52886.3522	p	473	0.00104927	–0.00011723	7
52887.5769	s	474.5	0.00114626	–0.00011735	6
52920.6400	p	515	–0.00003515	–0.00012059	3
52982.2775	s	590.5	–0.00088690	–0.00012663	8
53208.4209	s	867.5	–0.00084367	–0.00014880	9
53212.5011	s	872.5	–0.00265373	–0.00014920	9
53221.4850	s	883.5	0.00082416	–0.00015008	10
53228.4284	p	892	0.00480708	–0.00015076	10
53250.4661	p	919	–0.00034719	–0.00015292	10
53255.3663	p	925	0.00144075	–0.00015340	10

table continued on next page

Table 3. Recalculated eclipse timing residuals $(ETR)_2$ for KW Peg following simple linear least squares fit of residuals $(ETR)_1$ from the reference epoch and cycle number occurring between 1990 Sept 24 and 2011 Nov 08, cont.

Time of Minimum (HJD–2400000)	*Type*	*Cycle Number*	*$(ETR)_1$[a]*	*$(ETR)_2$*	*Reference**
53257.4052	s	927.5	–0.00066428	–0.00015360	10
53360.2722	s	1053.5	–0.00031753	–0.00016369	11
53589.6806	s	1334.5	–0.00088234	–0.00018618	3
53601.5201	p	1349	0.00078851	–0.00018734	12
53613.3551	s	1363.5	–0.00204064	–0.00018850	12
53617.4407	s	1368.5	0.00149931	–0.00018890	13
53627.6449	p	1381	0.00072419	–0.00018990	14
53659.4834	p	1420	–0.00045420	–0.00019302	12
53928.4864	s	1749.5	–0.00191649	–0.00021940	15
53966.4520	p	1796	0.00099004	–0.00022312	16
54002.3717	p	1840	–0.00099840	–0.00022664	16
54297.5015	s	2201.5	–0.00052501	–0.00025557	15
54384.4495	p	2308	0.00062092	–0.00026410	17
54755.5016	s	2762.5	–0.00191929	–0.00030047	18
54757.5431	p	2765	–0.00142432	–0.00030067	18
54759.5844	s	2767.5	–0.00116267	–0.00030087	18
54766.5239	p	2776	–0.00111309	–0.00030155	18
55000.4237	s	3062.5	–0.00046562	–0.00032448	19
55000.4243	s	3062.5	0.00013438	–0.00032448	19
55000.4254	s	3062.5	0.00123437	–0.00032448	19
55121.6584	p	3211	–0.00145411	–0.00033637	20
55146.5584	s	3241.5	–0.00171541	–0.00033881	21
55481.2842	s	3651.5	–0.00073951	–0.00037162	22
55842.5411	p	4094	–0.00169561	–0.00040704	18
55844.5806	s	4096.5	–0.00320063	–0.00040724	18
55850.7070	p	4104	0.00015096	–0.00040784	23
55857.2382	p	4112	0.00013488	–0.00040848	24
55868.6681	p	4126	0.00040674	–0.00040960	18
55873.5661	p	4132	–0.00000532	–0.00041008	18

Note: a. Eclipse Timing Residuals $(ETR)_1$ from linear elements (Kreiner 2004) for KW Peg.

** References: (1) De Young 1991; (2) BBSAG 1994; (3) Samolyk 2008; (4) Agerer and Hübscher 2003; (5) Zejda 2004; (6) Hübscher 2005; (7) Krajci 2005; (8) Kotková and Wolf 2006; (9) Pribulla et al. 2005; (10) Hübscher et al. 2005; (11) Zejda et al. 2006; (12) Hübscher et al. 2006; (13) Brát et al. 2007; (14) Dvorak 2006; (15) Parimucha et al. 2009; (16) Hübscher and Walter 2007; (17) Zasche et al. 2011; (18) Alton 2013 (present study); (19) Brát et al. 2011; (20) Diethelm 2010; (21) Samolyk 2010; (22) Hübscher 2011; (23) Diethelm 2012; (24) Hübscher and Lehmann 2012.*

Table 4. Spectral classification of KW Peg based upon data from various survey catalogs and present study.

Stellar Attribute	*Tycho-2*	*USNO-B1.0*	*USNO-A2.0*	*All Sky Combined*	*MPOSC3*	*2MASS*	*SDSS-DR8*	*Present Study*
(B–V)	0.903	0.728	0.945	0.785	0.805	0.804	0.838	0.733
Teff[a] (K)	5040	5470	4953	5320	5269	5272	5188	5574
Spectral Class[b]	K1	G8	K2	G9	G9	G9	K0	G8

Notes: a. Interpolated from Flower (1996). b. Estimated from Harmanec (1988).

Table 5. Selected geometrical and physical elements for KW Peg obtained during Roche model light curve fitting.

Parameter	*Unspotted Fit*	*Cool Spot 1*	*Hot Spot 2*
T_1 (K)[a]	5260	5260	5260
T_2 (K)	5046 ±25	5094 ±24	5128 ±25
q (m_2/m_1)[b]	0.911 ±0.021	0.911 ±0.015	0.914 ±0.016
A[a]	0.5	0.5	0.5
g[a]	0.32	0.32	0.32
Ω_1[b]	5.322 ±0.054	5.258 ±0.089	5.232 ±0.066
Ω_2[b]	5.126 ±0.098	5.125 ±0.073	5.131 ±0.075
i°[b]	78.3 ±0.21	78.3 ±0.17	78.4 ±0.20
$A_{S1} = T_{S1}/T$[d]	—	0.909 ±0.007	1.107 ±0.011
Θ_{S1} (spot co-latitude)[d]	—	6 ±1.28	32.5 ±10
φ_{S1} (spot longitude)[d]	—	354.9 ±8.3	0 ±8
r_{S1} (angular radius)[d]	—	38.7 ±0.71	13.47 ±0.44
r_1(back)[e]	0.2315 ±0.0092	0.2351 ±0.0067	0.2368 ±0.0074
r_1(side)[e]	0.2281 ±0.0091	0.2315 ±0.0066	0.2331 ±0.0073
r_1(pole)[e]	0.2256 ±0.0090	0.2289 ±0.0065	0.2304 ±0.0072
r_1(point)[e]	0.2328 ±0.0093	0.2366 ±0.0068	0.2384 ±0.0074
r_2(back)[e]	0.2284 ±0.0091	0.2285 ±0.0065	0.2288 ±0.0071
r_2(side)[e]	0.2245 ±0.0090	0.2247 ±0.0064	0.2250 ±0.0070
r_2(pole)[e]	0.2219 ±0.0089	0.2221 ±0.0064	0.2224 ±0.0069
r_2(point)[e]	0.2299 ±0.0092	0.2301 ±0.0066	0.2304 ±0.0072
$\chi 2$ (B)[c]	0.013134	0.013362	0.012997
$\chi 2$ (V)[c]	0.013006	0.013194	0.012617
$\chi 2$ (I_c)[c]	0.054050	0.052406	0.052273

Notes: a. Fixed elements during DC. b. Variability (±S.D.) from heuristic $\chi 2$ scanning in PHOEBE. *c. $\chi 2$ from* PHOEBE *(Prša and Zwitter 2005). d. Error estimates from* WDWINT *v5.6a (Nelson 2009a). e. Formal error estimates from numerical methods according to* PHOEBE *0.32 manual (Prša and Harmanec 2010).*

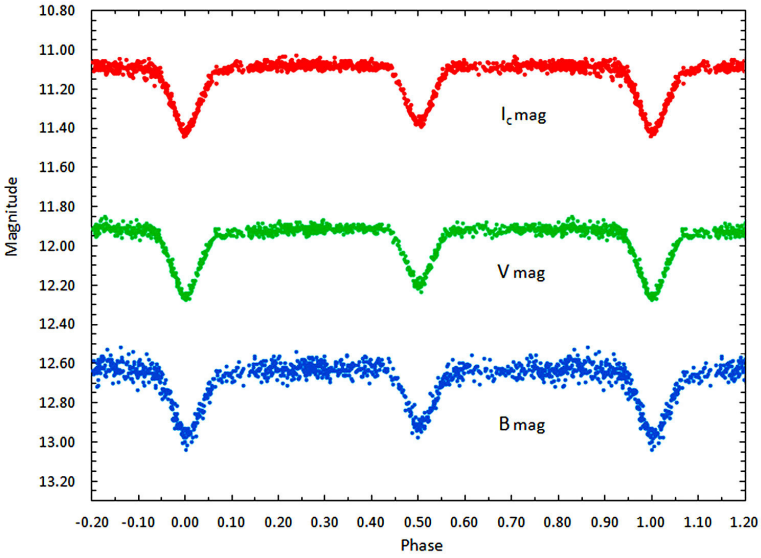

Figure 1. Folded CCD light curves for KW Peg obtained between October 8 and October 31, 2008. The top (I_c), middle (V), and bottom curve (B) shown above were reduced to magnitudes from the MPOSC3 catalogue using MPO CANOPUS.

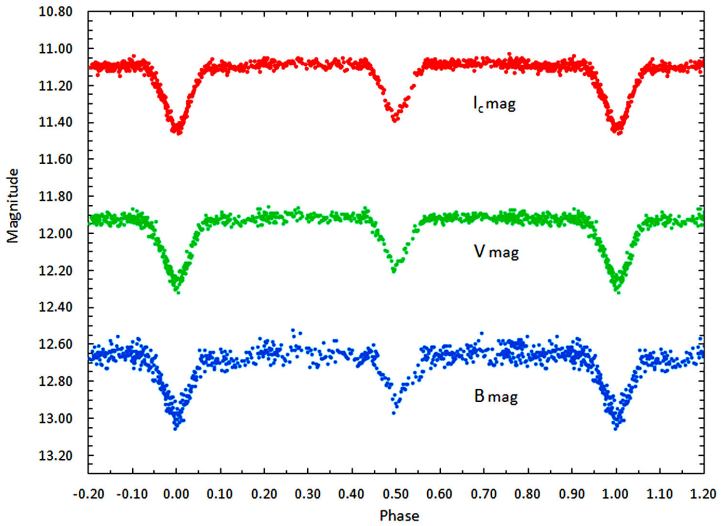

Figure 2. Folded CCD light curves for KW Peg obtained between October 6 and November 8, 2011. The top (I_c), middle (V), and bottom curve (B) shown above were reduced to magnitudes from the MPOSC3 catalogue using MPO CANOPUS.

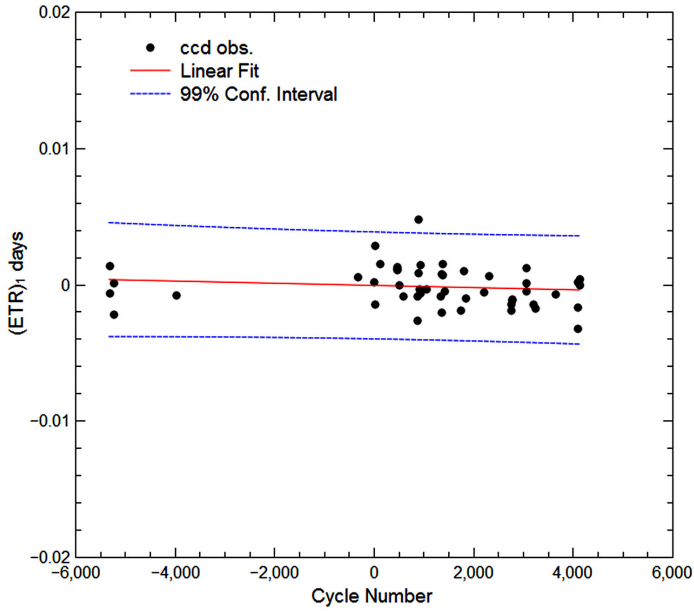

Figure 3. Linear regression fit of all CCD time-of-minimum residuals $(ETR)_1$ reported for KW Peg between 1990 and 2011. The eclipse timing residuals $(ETR)_2$ after curve fitting do not exhibit any other underlying periodicity that can be determined at this point.

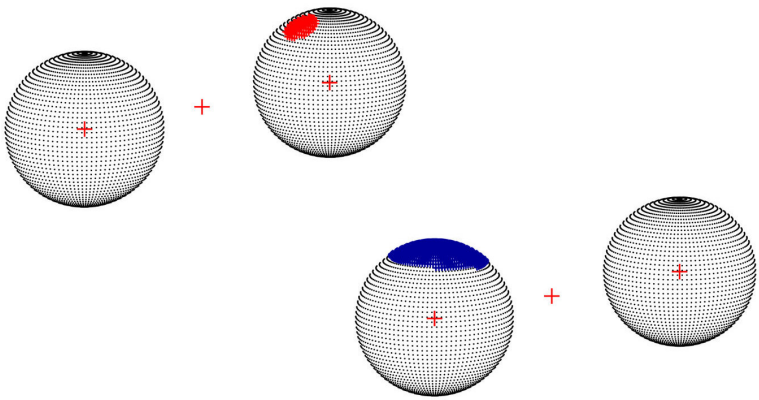

Figure 4. 3-D spatial representations of KW Peg showing the location of a putative hot spot on secondary star (top) or alternatively, a cool polar crown on the primary star (bottom).

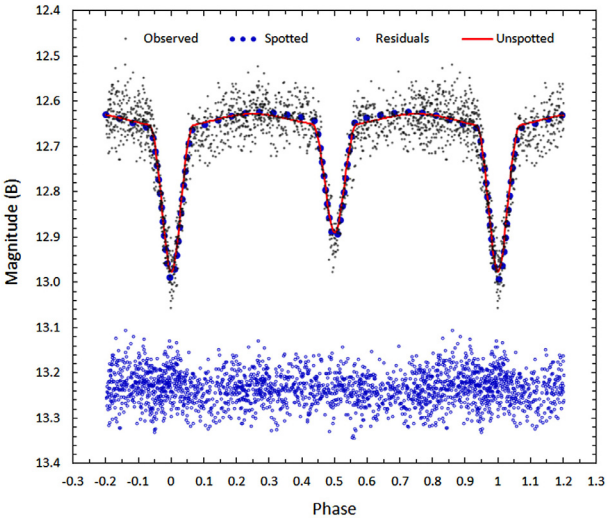

Figure 5. Synthetic fit of B bandpass light curve for KW Peg (2008 and 2011) collected at UO using an unspotted (solid-line) and spotted (dotted-line) Roche model which incorporates a cool polar crown on the more massive star. Spotted residuals are offset by a constant value to keep the y-axis on scale.

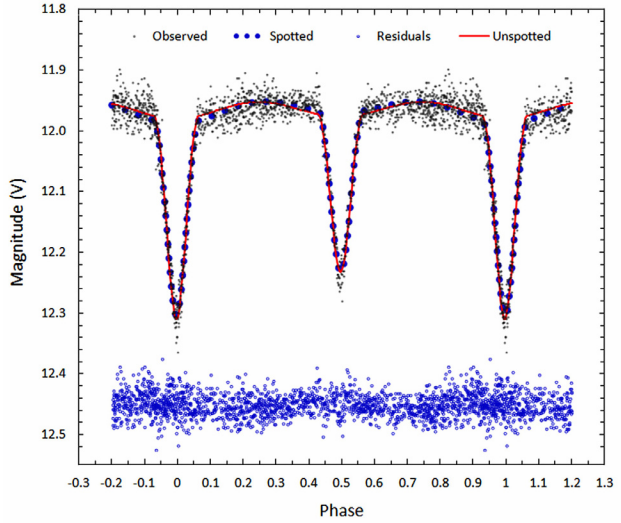

Figure 6. Synthetic fit of V bandpass light curve for KW Peg (2008 and 2011) collected at UO using an unspotted (solid-line) and spotted (dotted-line) Roche model which incorporates a cool polar crown on the more massive star. Spotted residuals are offset by a constant value to keep the y-axis on scale.

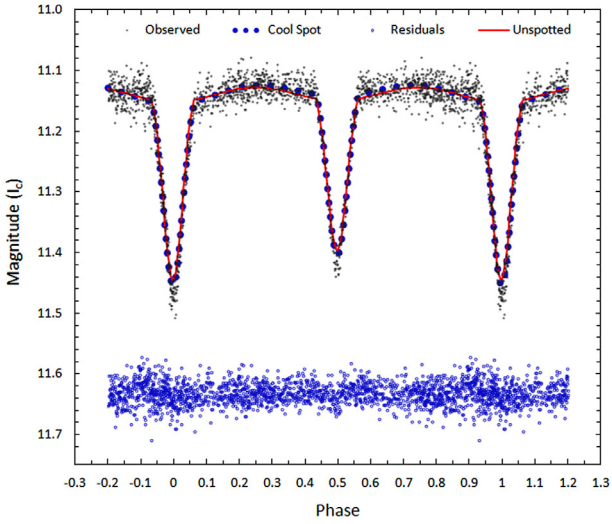

Figure 7. Synthetic fit of I_c bandpass light curve for KW Peg (2008 and 2011) using an unspotted (solid-line) and spotted (dotted-line) Roche model which incorporates a cool polar crown on the more massive star. Spotted residuals are offset by a constant value to keep the y-axis on scale.